Vibration monitoring for the detection of tool failure in broaching machines

M. Troncossi, S. Rosa, A. Rivola, A. Martini
University of Bologna, Department of Industrial Engineering (Forlì Campus),
via Fontanelle 40, I-47121, Forlì, Italy
e-mail: **marco.troncossi@unibo.it**

Abstract
Condition based maintenance of machine tools is critical in order to improve maintenance efficiency, keep high production rate and minimize the environmental impact. Vibration monitoring is a very popular method adopted when it comes to assessing the health conditions of sub-systems such as feed axis, gearbox or single components as the tool itself. Most papers of recent literature are mainly focused on traditional machining process like milling, turning and drilling, whereas to the authors' best knowledge little attention seems to be addressed to broaching process. Aiming to contribute to fill this gap, the present work illustrates the experimental campaign that was conducted on a broaching machine both in its healthy condition and in a few failure states. The experimental results of some different analysis techniques that were investigated confirm the possibility of distinguishing between healthy and faulty conditions of the tool; yet, further investigations are required in order to improve accuracy and robustness of the procedure.

1 Introduction

Predictive maintenance, sometimes called "on-line monitoring" or "condition-based maintenance", is a maintenance strategy that uses the actual operating condition of plant equipment and systems to optimize total plant operation [1]. As a result, predictive maintenance can avoid unnecessary equipment replacement, save costs, and improve process safety, availability, efficiency and environmental sustainability [2]. Despite all the technological developments, an automated manufacturing is not achievable without reliable condition monitoring systems [3]. Machine tools can be considered the backbone of modern manufacturing due to their complex machining capabilities. Obviously, as machine tools gain complexity, so do their maintenance requirements. As the maintenance of those systems can be very expensive, the maintenance actions must be optimized in order to maximize economic profitability. Usually the most critical systems are feed drives, that are composed of an actuator and guideways or slides. Monitoring the health state of feed drives can prove useful in optimizing maintenance actions [4]. Ball-screw systems are very common in industrial applications and due to high-dynamics functioning, the ball screw is usually in gradual wear state, affecting the resulting product quality. Condition monitoring of ball-screw systems can be accomplished through analysis of vibration signals [5, 6] and/or motor current consumption [5], with particular attention to wear detection and performance degradation. However, while these methods are sensor-based, meaning that the installation of external sensors is required, wear detection is feasible even by analysis of internal control signals [7] resulting in a less expensive set-up. Along with ball-screw drives, bearings are one of the essential components of a machine tool whose failure is one of the most prevalent reasons for machine failure. Fault detection of bearings can be a challenging task, especially under operating conditions in an industrial environment. A survey of methods for condition monitoring of bearings in machine tools can be found in [8], whereas an example of fault detection method based on the analysis of both vibration and acoustic signals is reported in [9]. Among other systems, gearboxes are usually found in tool machines as speed reduction between motor and the tool is often required. An effective way of assessing the health conditions of a machine tool gearbox by means of built-in position sensors is presented in [10]. Finally, since tool

failure represents the 20% of machine tool downtime [11], an accurate Tool Condition Monitoring (TCM) is essential in order to increase productivity, increase product quality and reduce maintenance costs. TCM has received a lot of attention in the last years [12–14], however the majority of these works are mainly focused on traditional machining process like milling, turning and drilling while giving very little attention to the broaching process, likely due to the high initial investment costs [16] with respect to the relatively low cost per part. To the authors' best knowledge, the only example of work about condition monitoring of a broaching machine can be found in [15]. The aim of the present study is to explore predictive maintenance strategies for TCM on a broaching machine based on vibration signals, in order to assess the feasibility of its implementation as a real business optional service. An experimental campaign is conducted on a test facility in order to assess the effectiveness of different kinds of analysis. In particular, faults are artificially induced on a broaching machine tool during the test stage with the help of the manufacturer company. The vibration signals related to the faults and the healthy conditions are measured by using four triaxial accelerometers arranged along the machine basement. Different types of fault were investigated and the detection performance provided by the different procedures are evaluated and compared.

2 Materials and method

The experiments were conducted on a broaching machine made for production of lock plugs, more specifically to derive the profile where the key is inserted. The machine main axis controls a transmission chain which drags 16 workpiece carriers, fixed to the chain with a relative distance of 311mm, whereas the broach tool is fixed. The latter is made of high-speed steel and is 1600mm long, yet divided in 16 separate sectors with 10 teeth each thus resulting in a 10mm tool pitch. The chain maximum speed is 11.41 m/min corresponding to a production rate of 2200 pc/h.
The machine is quite flexible and the workpieces that can be machined may vary to a certain extent: in the tests performed, lock-cylinders made of a brass alloy, 39.35mm long and with a 14mm diameter have been targeted. Being the first laboratory test performed on the (unknown) machine, a redundant sensor setup was arranged, with 4 triaxial accelerometers placed on the machine basement, almost equidistant along the entire length of the tool (Fig. 1). It is worth observing that for practical implementation in industry, a highly simplified setup would be required for the sake of overall cost sustainability (e.g. up to 2 single-axis sensors at most). The signals were measured with sampling frequency Fs = 8192 Hz for a duration T_s = 30 s; all the measurements were repeated three times for the sake of data reliability.

The tests were carried out in many different operating conditions in order to possibly better interpret the experimental data. In this paper, for the sake of synthesis, only the underlined conditions in the following list will be referred to:

- transmission chain velocity:
  - 10.37m/min (production rate 2000pc/h);
  - 94.70m/min (1826pc/h);
- carriers loaded with workpiece:
  - all the carriers (real operating condition);
  - no carrier (in order to get the vibration signature of the machine in no-load condition);
  - just one carrier;
  - two consecutive carriers;
  - 8 carriers (in the sequence: loaded-empty-loaded-empty-…);
- tool condition:
  - healthy, i.e. no faults, hereinafter conventionally referred to as *NF*;
  - 1 broken tooth, *F1* (the first tooth of the fifteenth broach segment was removed, Fig. 2a);
  - 3 broken teeth, *F2* (the first 3 teeth of the fifteenth broach segment were removed, Fig. 2b).

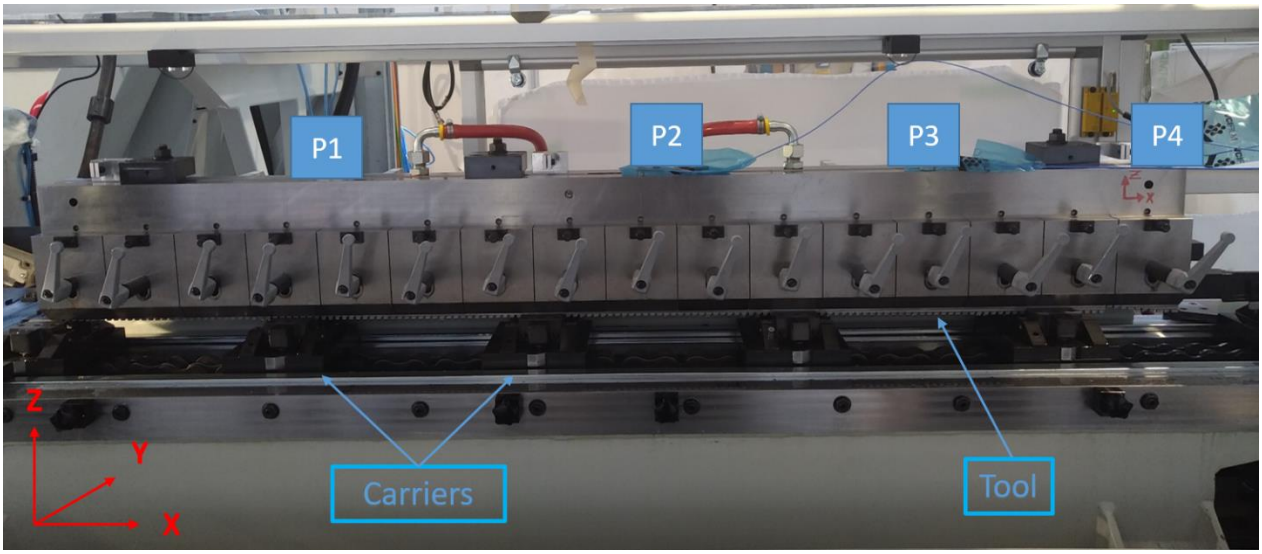

Figure 1: Machine front view and sensors locations (P_1 – P_4).

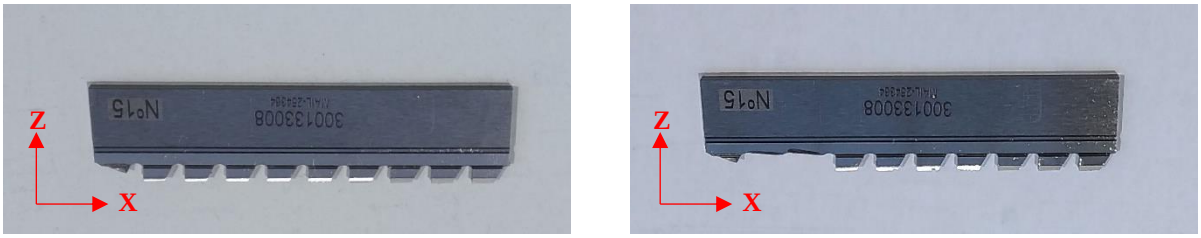

(a) (b)

Figure 2: Induced tool fault: one tooth broken (a), three teeth broken (b).

3 Signal processing and results

Preliminary analyses to check data repeatability and to understand physical events in the machine functioning whose effects are visible in the vibration signals were performed considering *NF* tool health state and the combination of the conditions non-underlined in the list of Section 2. The results are not discussed in this report.

Focusing on the comparison of *NF* vs. *F1* and *F2* tool states, three kinds of analysis are reported and the corresponding results discussed in this Section. In particular, the very standard technique used at first and based on Time-, Frequency-, and Time-Frequency domains analyses of the measured signals did not provide any evidence of fault presence (Section 3.1). Hence, limited signal blocks were properly extracted from the measures and the investigation of their mutual correlations was performed (Section 3.2), leading to promising results. Finally, based on the latter, the analysis of cross-correlations was enforced through the implementation of classification algorithms based on Machine Learning (Section 3.3).

3.1 Analysis-1: standard processing of measured accelerations

The occurrence of severe damages was expected to alter considerably the dynamic response of the machine, possibly exciting to a certain extent the first mode(s) of the structure due to impact-like contact of the workpiece with the first healthy tooth remained after the removal of 1 (*F1*) or 3 (*F2*) teeth, resulting in a higher level of vibration. On the contrary, based on all the standard analyses performed (statistical parameters calculation, analyses of the Fourier and Short-Time-Fourier Transforms…), even in the extreme

case *F2* the vibration signature retrieved at the machine basement proved basically identical to the *NF* one. As an example, Table 1 reports the RMS values of all the signal acquired for the two conditions *NF* and *F2*, showing that no discrimination can be reliably done based on the vibration severity. In Fig. 3, still as an example, the timeseries of signal P_{4Y}, being P_4 the position closest to the damage, are plotted: they clearly appear very similar. In particular, large amplitude peaks can be observed as dominating the machine response. These spikes are probably due to the impact between the cam-based mechanism for loading the workpieces on the carriers and the carriers themselves: indeed, their period is about 1.8s which corresponds to the feed rate when the machine is operated for a production of 2000 pc/h.

Table 1: RMS values [g] of the signals computed for conditions *NF* and *F2*

	P_{1X}	P_{1Y}	P_{1Z}	P_{2X}	P_{2Y}	P_{2Z}	P_{3X}	P_{3Y}	P_{3Z}	P_{4X}	P_{4Y}	P_{4Z}
NF	0.14	0.28	0.07	0.14	0.20	0.07	0.08	0.20	0.07	0.24	0.26	0.12
F2	0.13	0.27	0.08	0.14	0.20	0.07	0.08	0.20	0.07	0.22	0.25	0.13
Δ%	-4.3%	-5.0%	2.7%	1.5%	-1.5%	2.8%	1.2%	-1.0%	1.4%	-7.1%	-1.2%	2.5%

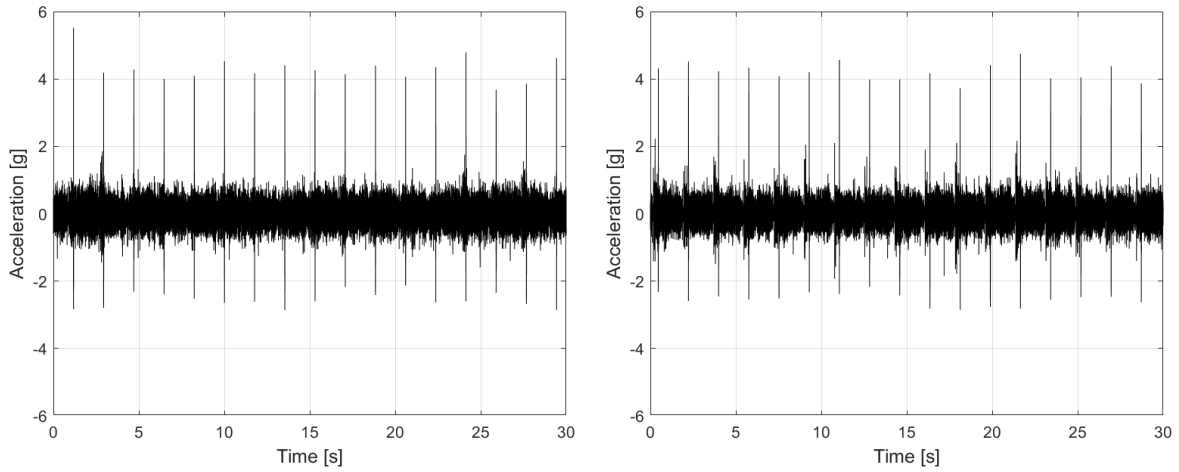

(a) (b)

Figure 3: Signals acquired in healthy tool condition *NF* (a), faulty condition with three teeth broken *F2* (b).

The same conclusions hold true for all the other signals and signal parameters as well as for the spectral analyses, which are not reported here. The apparent insensitivity of the machine vibration levels with respect to the presence of faults may be reasonably due to the very high stiffness of the basement which has to guarantee strict machining tolerances and accuracy. Since an alternative setup arrangement was not possible (i.e. with sensors placed over the tool or on the moving parts), a different approach was investigated.

The next step was trying to exclude the contribution of the large peaks in the computation of the statistical parameters by extracting the segments of signal between the spikes. As a result, 16 data blocks of a duration $T_b \approx 1.76$s were extracted from the original signals for each channel and each test, and are conventionally named *extracted blocks* hereafter. Figure 4 shows the results of statistical analysis following this procedure (limited to channels in the Y direction). In particular, the RMS and kurtosis values are reported as the arithmetic mean of the parameters computed for each block extracted from an acquisition; the corresponding standard deviation σ is also reported through vertical segments indicating ±σ intervals, which proves the data repeatability and thus an acceptable reliability of results (as also shown in Fig. 5 where, as an example, the 16 PSDs of the extracted blocks are basically superimposed). In Fig. 4 it can be perceived that no big differences can be observed when moving from condition *NF* to condition *F2*, that is to say the introduction of the fault does not affect significantly the statistical parameters computed even neglecting the dominant peaks of the entire acquisition. Unfortunately, the comparison of the PSDs computed as average over the 16 extracted blocks for a given acquisition (resolution $\Delta f = 1/T_b \approx 0.57$Hz), is not able to reveal any difference neither in the Frequency domain (e.g. see the PSDs of P_{4Y} extracted blocks in Fig. 6).

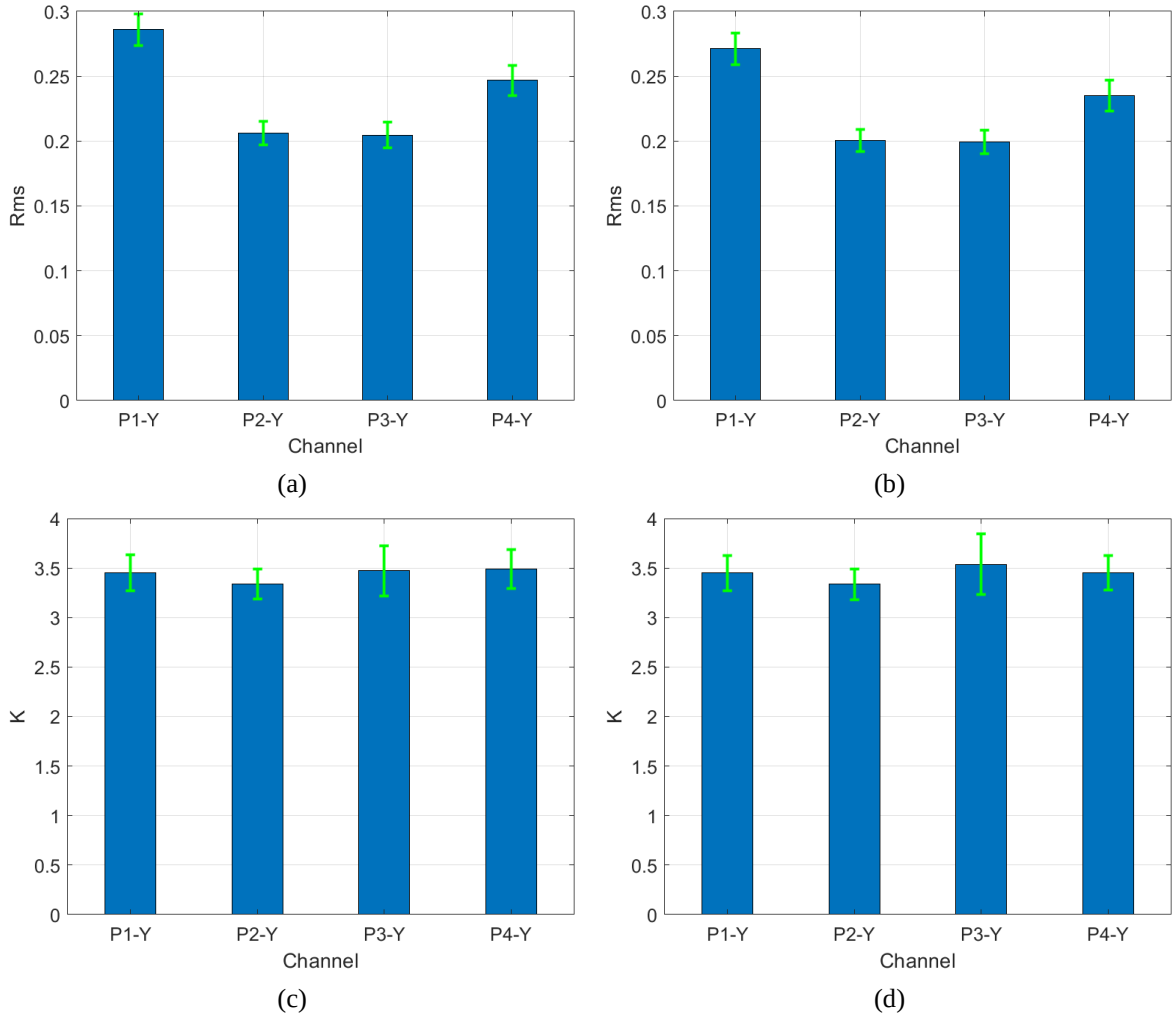

Figure 4: Mean RMS value in *NF* (a) and *F2* (b) conditions; mean kurtosis value in *NF* (c) and *F2* (d) conditions for signals in Y direction (± standard deviation intervals are indicated by the green vertical bars).

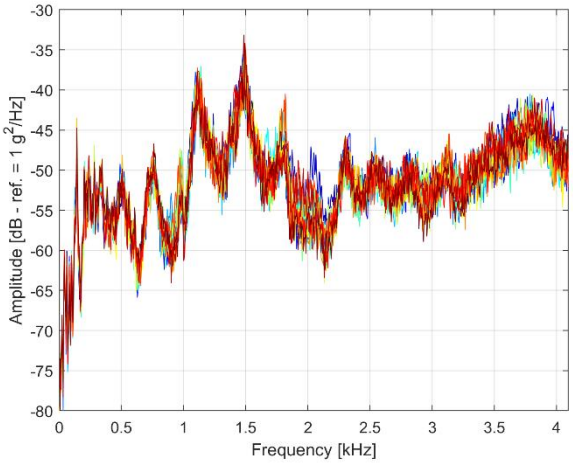

Figure 5: PSD of the 16 extracted blocks from channel P_{4Y} in *NF* condition.

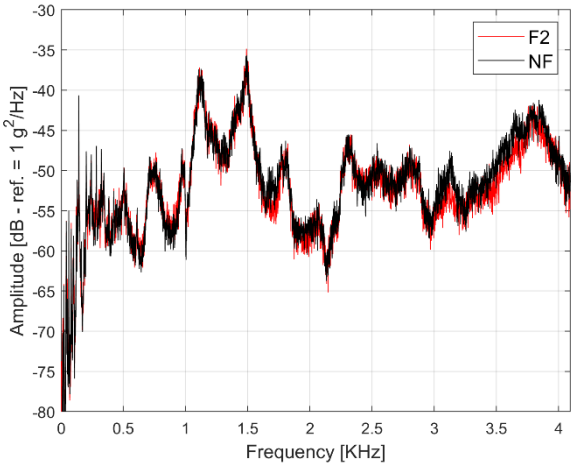

Figure 6: average PSD of channel P_{4Y} extracted blocks, computed in different *NF* and *F2* conditions.

3.2 Analysis-2: signal cross-correlation

Since the basic analysis techniques did not perform as expected, an exploratory approach based on the cross-correlation functions and their statistical analysis was undertaken, based on idea of the authors who had met similar problems in a previous application [17]. In a few words, auto- and cross- correlations analysis performed for monitoring the possible presence of leaks in a water distribution pipeline had proven that the presence of faults would make the signal correlation functions more similar to the trend of the auto-correlation of Gaussian white noise than in the case of healthy conditions (in particular as for the presence and distribution of spikes, which can be quantitatively evaluated through the kurtosis coefficient of the function signals). The processing followed five main steps:

1. the repeatability of the extracted signal blocks was verified (Section 3.1);
2. every entire acquisition was replaced with one representative extracted block, arbitrarily chosen as the one having the lowest RMS value;
3. the representative extracted blocks were grouped in three classes, featuring the same direction of the corresponding channels that they were from;
4. the cross-correlations between each representative extracted blocks belonging to the same group were computed;
5. the statistical parameters of the cross-correlation functions were computed and compared. The most meaningful parameter proved to be the kurtosis coefficient, which is the only one feature that will be discussed in the following.

A flowchart summarizing these steps as well as the combinations of signals used to compute the cross-correlation functions is presented in Fig. 7. The process proposed above was repeated for both a *NF* and a *F2* conditions so as to compute the corresponding percentage variation of the kurtosis values.

Figure 8 shows the different plots of the normalized cross-correlation functions between representative extracted blocks from channels P_{1Y} and P_{4Y}, for *NF* and *F2* conditions, respectively, whereas Fig. 9 reports the percentage variation of the kurtosis value for each combination of signal defined in Fig. 7 when moving from the *NF* condition to *F2*. Regarding Fig. 9, large positive increases of the kurtosis values can be observed when the fault is introduced, especially for the cross-correlation between sensors P_1 and P_4 in Y direction. This result makes sense as P_1 and P_4 are the sensors further apart and P_4 is the closest one to the induced fault. As a consequence, it could be reasonably expected that the related signals features the lowest degree of similarity when the fault is introduced and therefore a significant change in the cross-correlation function. Percentage variations of kurtosis values computed for the cross-correlation functions are significantly large and positive in both the Y and Z directions and thus they might be targeted as a meaningful index for monitoring the broach tool health condition. It is worth noting that, unexpectedly, the kurtosis variation in the X direction – the same as the machining process flow – is completely different from the other ones.

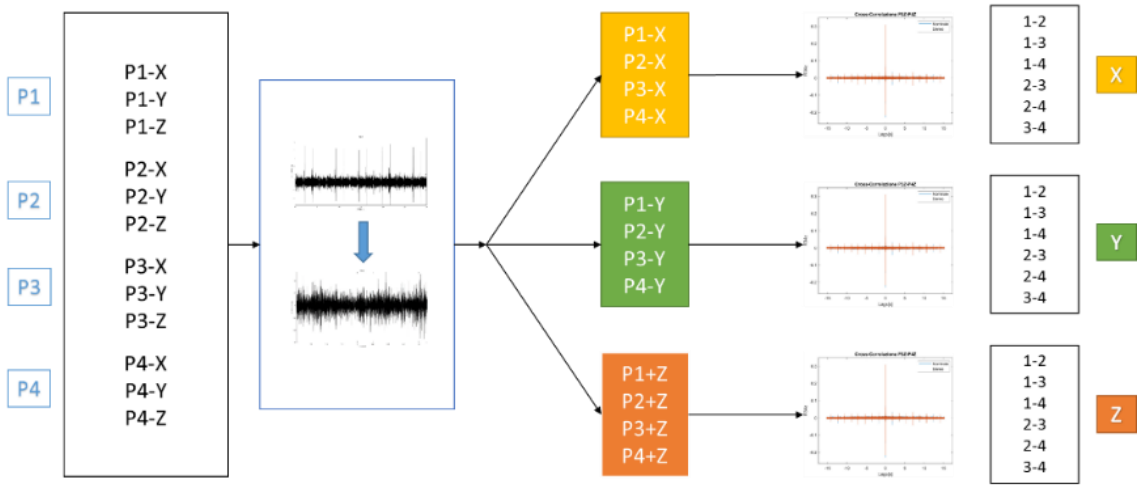

Figure 7: Work flow of Analysis-2 procedure.

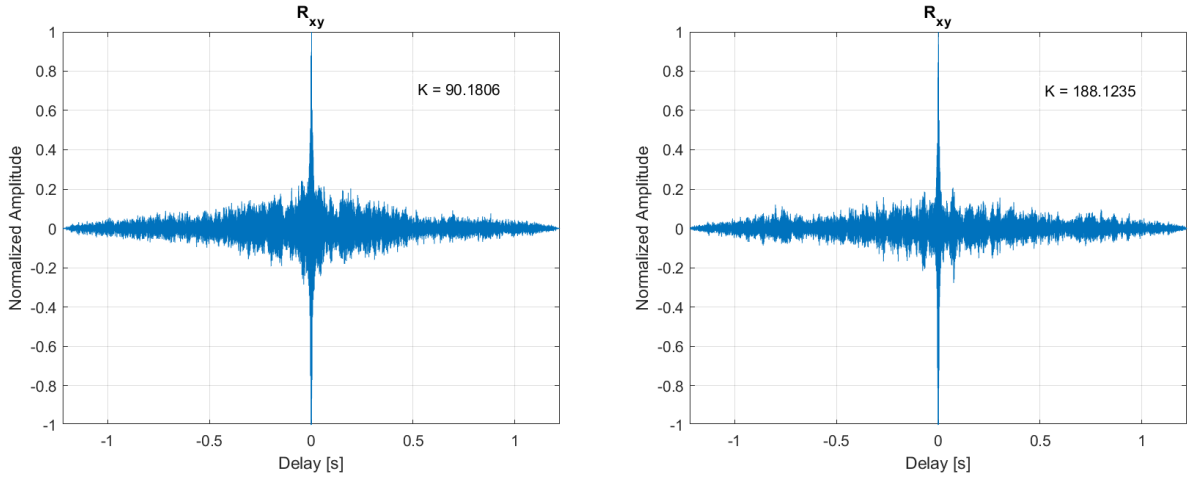

(a) (b)

Figure 8: Normalized cross-correlation functions of the representative extracted blocks for channel P_{1Y} and P_{4Y} in *NF* (a) and *F2* conditions (b).

3.3 Analysis-3: machine learning

Given the promising results obtained at Section 3.2 yet aiming at more robust findings, the implementation of Machine Learning algorithms was undertaken. Based on the same previous work-flow, different combinations of signals were initially investigated in order to build the data-set for both the training and the test stages of the three tested algorithms, namely Random Forest, Support Vector Machine, and k-Nearest Neighbours. Regarding performance, usually the larger the training set the better the accuracy of the algorithm and therefore the cross-correlation functions were particularly suitable to get a significant size of the data-set. Nevertheless, from the huge amount of preliminary results (here not reported for obvious reasons), it turned out quite surprisingly that reducing the analysis to just one channel, namely P_{4X}, allowed for increased accuracy and thus it was.the only one considered to compute features and feed the algorithms.

The features were computed both for (i) the extracted blocks from the "physical" signal and (ii) the cross-correlation functions of the 16 extracted blocks . Going into details, as the training set needs for "observations" of both conditions, the channel P_{4X} coming from *NF* and *F2* conditions were employed for building the training set. Hence, a total of 16 blocks were extracted from each signal and related one to another following the scheme shown in Fig. 10: every block was correlated with all the other blocks extracted from the same signal avoiding repetitions and auto-correlations, leading to a total number of 240

observations. Finally, the features were computed in different domains. A first set was computed directly on the cross-correlation functions while the second set was computed as the ratio between the parameters computed for each extracted block ("physical" time signals) following the same combinations of Fig. 10 – employed for the computation of the cross-correlation functions – in order to keep consistency in the feature space. The parameters computed on the segments came both from the Time domain (statistical parameters) and the Frequency domain (amplitude peak and corresponding frequency in the PSD). The feature vectors obtained for every observation were then labelled and fed into the classification stage as shown in Fig. 11.

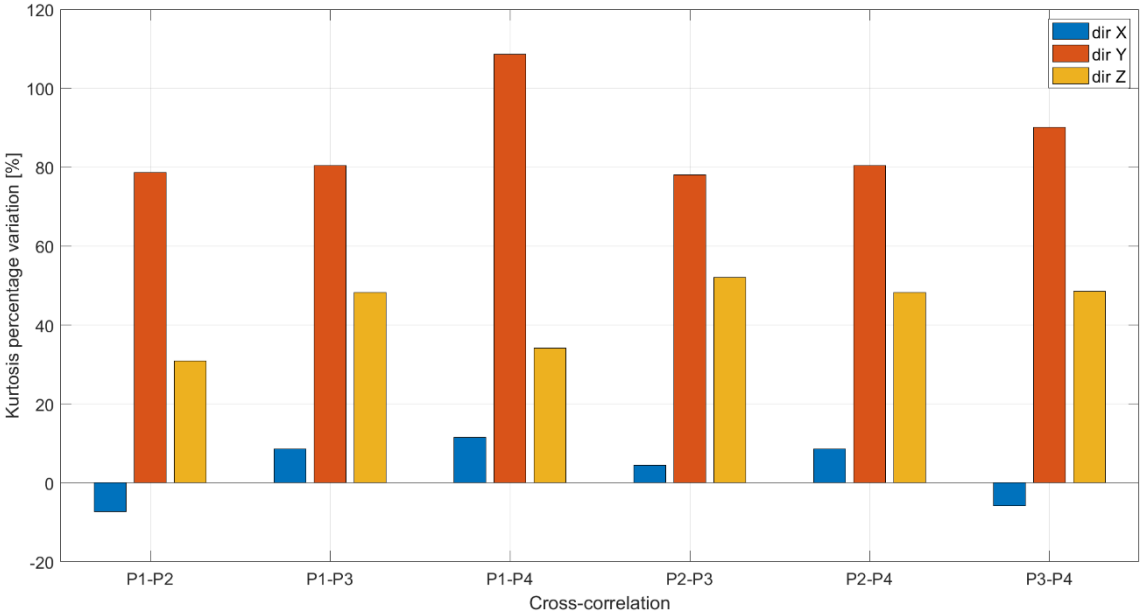

Figure 9: Percentage variation of the kurtosis value computed over the normalized cross-correlations.

The algorithm selected as the most suitable for the present application is a *k-Nearest Neighbour* (*kNN*) with k equal to 10, distance set to Euclidean, weights being proportional to the distance and feature normalization. This algorithm is capable of categorizing objects based on the classes of their first k nearest neighbours in the dataset assuming that objects near each other are similar. Basically, the algorithm predictions assume that objects near each other are similar. At first, the tests were conducted by comparing *NF* condition with the case *F2* following the results obtained in Section 3.2. This was done in order to investigate a basic capability of the implemented procedure of detecting an induced fault even if being far from a real-world scenario. The features employed were basically Mean Absolute Deviation (MAD), Inter Quartile Range (IQR), Root Mean Square (RMS), Crest Factor (CF), Skewness and Kurtosis, Range, Amplitude Peak and the corresponding location and the mean normalized frequency. These features were computed on the cross-correlations and on the extracted blocks (from the time signals) yet substituting the last two with the amplitude peak and the corresponding frequency of the PSD. Figure 12 shows the performance of the algorithm in the validation stage and test stage, respectively, by means of the so-called *confusion matrices* that give the specific accuracy for each class rather than the overall accuracy. Basically, the confusion matrix shows for each class the accuracy reached, usually called *True Positive Rate (TPR),* and the miss classification error called *False Negative Rate (FNR)*. The rows of the confusion matrix correspond to the true class and the columns correspond to the predicted class. Diagonal and off-diagonal cells correspond to the percentage of correctly and incorrectly classified observations, respectively. A plot of both the training set and test set in the feature space limited to two dimensions (i.e. two features) is shown in Fig. 13 where the green points are associated with healthy state and the red ones with the fault presence.

Finally, the proposed procedure was tested on the less severe damage condition, namely one tool tooth broken (*F1*). This was done with the purpose of simulating a real-world scenario and so checking the feasibility of the procedure as a real business option. Figure 14 shows the results obtained following the same procedure as before. As expected, the overall accuracy reached by the algorithm decreased, due to the rise of misclassified observations while keeping a high *TPR* for the faulty condition.

blocks	1	...	*j*	...	16
1	0	0	0	0	0
⋮	...	0	0	0	0
i	*i*-1	...	0	0	0
⋮	...	...	...	0	0
16	16-1	...	16-*j*	...	0

Figure 10: Scheme for computing the cross-correlation functions among the extracted blocks.

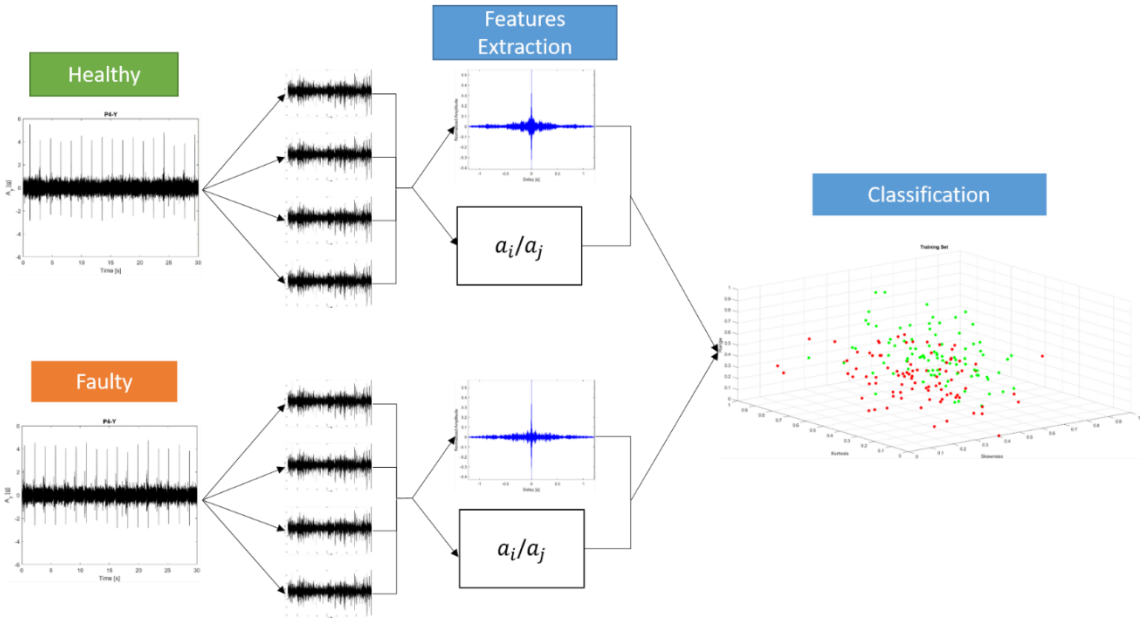

Figure 11: Analysis-3 work flow

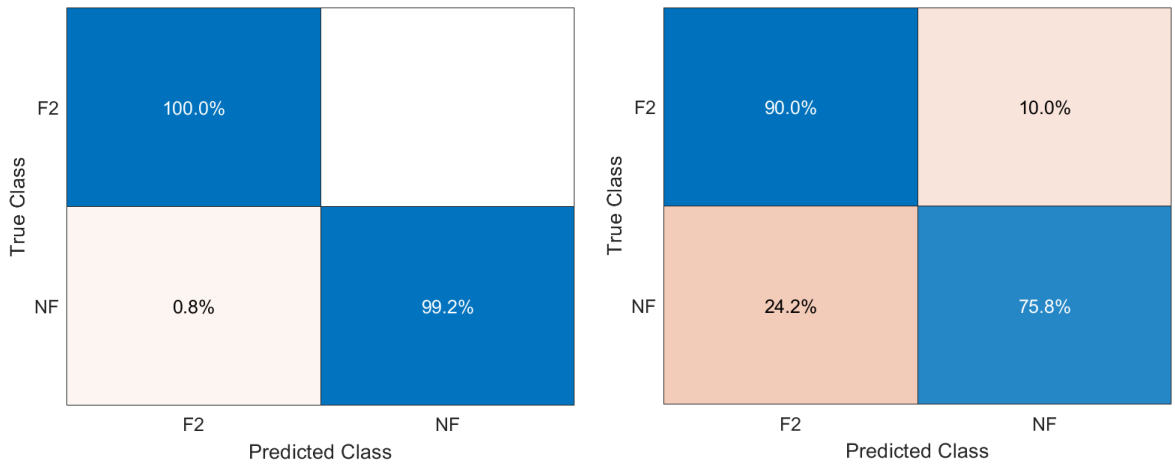

(a) (b)

Figure 12: Performance of the proposed procedure when comparing conditions *NF* and *F2* for validation data (a) and test data (b).

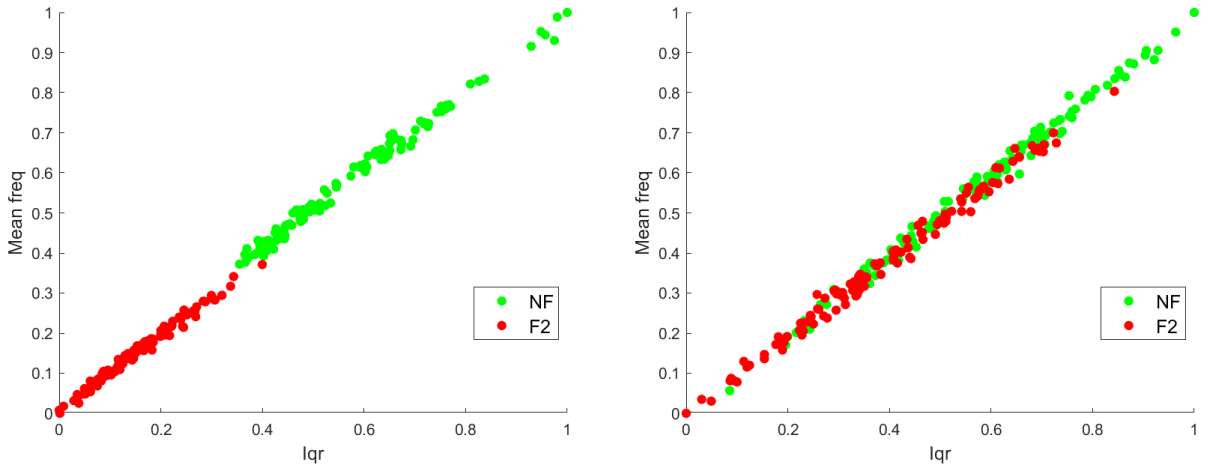

(a) (b)

Figure 13: Data sets used for training (a) and test (b) stages when comparing conditions *NF* and *F2*.

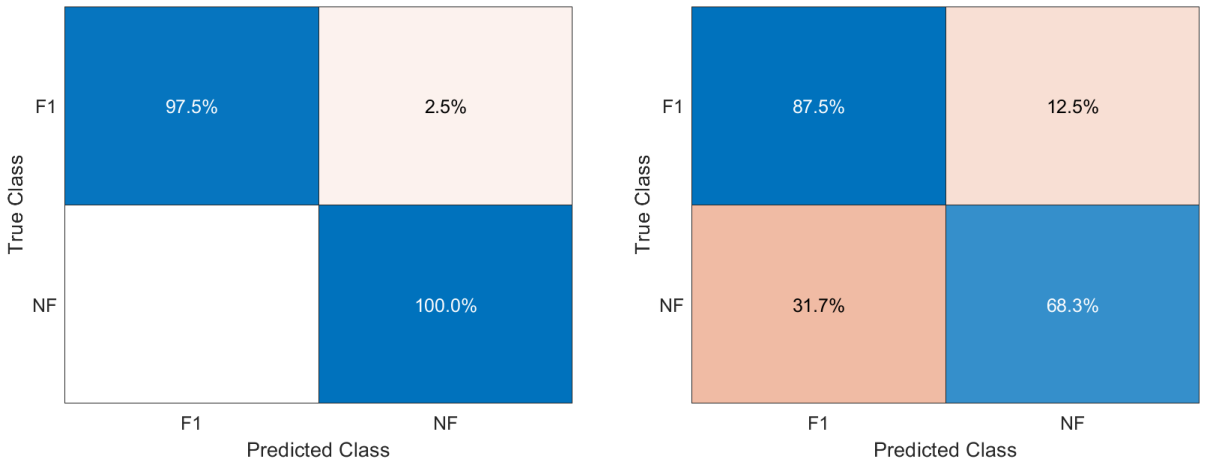

(a) (b)

Figure 14: Performance of the proposed procedure when comparing conditions *NF* and *F1* for validation data (a) and test data (b).

4 Conclusion

This paper presented the investigation of experimental vibration signals in order to define a method for the assessment of tool condition. The basic techniques have proven ineffective to detect a faulty condition from the accelerometer signals and consequently an alternative approach was undertaken. Specifically, the kurtosis value of the cross-correlation functions computed among limited data blocks properly extracted from the overall time signals acquisitions led to good results, showing a large increase with respect to the broach healthy condition when a fault was artificially induced on some tool teeth. Morevoer, in order to reach higher accuracy and robustness a machine learning k-NN algorithm was implemented, validated and tested on data coming from different tests, while computing the features both on the above mentioned cross-correlation functions and the time signals themselves. The experimental results showed high accuracy when trying to recognize observations associated with faulty conditions whereas the healthy state identification resulted in lower accuracy and this task keeps challenging. Hence, further investigations are needed in order to improve accuracy and robustness of the algorithm.

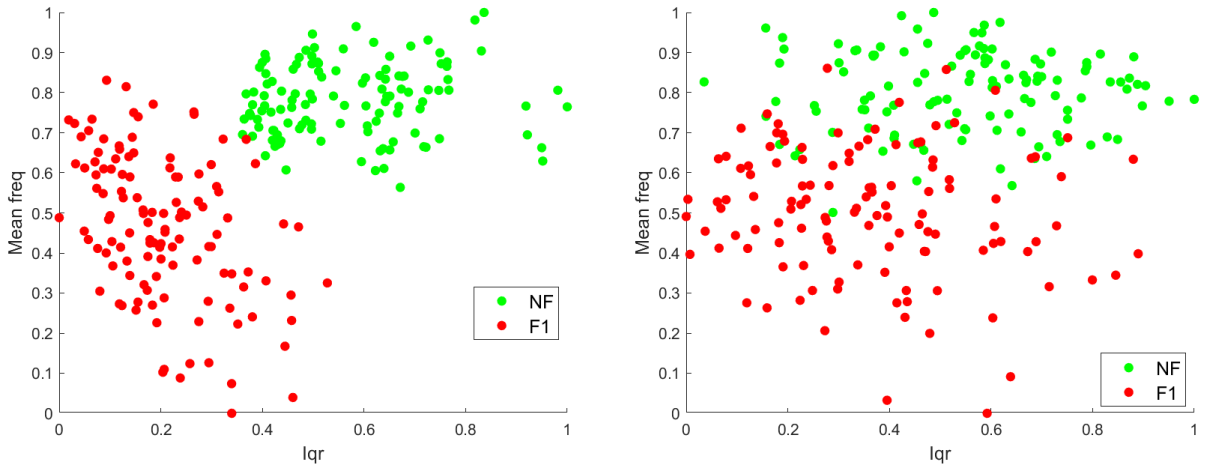

(a) (b)

Figure 15: Data sets used for training (a) and test (b) stages when comparing conditions NF and F1.

References

[1] R. K. Mobley, *An Introduction to Predictive Maintenance*, Butterworth-Heinemann, 2002.

[2] H. M. Hashemian, "State-of-the-Art Predictive Maintenance Techniques," *IEEE Transactions On Instrumentation and Measurement*, vol.60, no. 1, pp. 226-236, 2011.

[3] D. Goyal, and B. S. Pabla, "Condition based maintenance of machine tools - A review," *CIRP Journal of Manufacturing Science and Technology*, no. 10, pp. 24-35, 2015.

[4] Q. Butler, D.Stephenson, Y. Ziada, and S. A. Gadsden, "Condition Monitoring of Machine ool Feed Drives: A Review," *Journal of Manufacturing Science and Engineering*, vol. 144, no. 10, 2022.

[5] P. Jia, Y. Rong, and Y. Huang, "Condition monitoring of the feed drive system of a machine tool based on long-term operational modal analysis," *International Journal of the Machie Tools and Manufacture*, vol. 146, 2019.

[6] W. Lee, J. Lee, M. S. Hong, S-H. Nam, Y. Jeon, and M. G. Lee, "Failure Diagnosis System for a Ball-Screw by Using Vibration Signals," *Shock and Vibration*, 2015.

[7] X. Tiandong, S. Kehne, T. Fujita, A. Epple, and C. Brecher, "Condition Monitoring of Ball-Screw Drives Based on Frequency Shift," *IEEE/ASME Transactions on Mechatronics*, vol. 25, no. 3, pp. 1211-1219, 2020.

[8] S. Schwendmann, Z. Amjad, and A. Sikora, "A survey of machine-learning techniques for condition monitoring and predictive maintenance of bearings in grinding machines," *Computers in Industry*, vol. 25, 2021.

[9] M. Iqbal, and A. K. Madan, "CNC Machine-Bearing Fault Detection Based on Convolutional Neural Network Using Vibration and Acoustic Signal," *Journal of Vibration Engineering &Technologies*, pp.1-9, 2022.

[10] Y. Zhou, T. Tao, X. Mei, G. Jiang, and N. Sun, "Feed-axis gearbox condition monitoring using built-in position sensors EEMD method," *Robotics and COmputer-Integrated Manufacturing*, vol. 27, pp. 785-793, 2011.

[11] S. Y. Liang, R. L. Hecker, and R. G. Landers, "Machining Process Monitoring and Control: The State-of-the-Art," *Journal of Manufacturing Science and Engineering*, vol. 126, no. 2, pp. 297-310, 2004.

[12] G. Byrne, D. Dornfeld, I. Inasaki, G. Kettler, W. Konig, and R. Teti, "Tool COndition Monitoring (TCM) - The Status of Research and Industrial Application," *CIRP Annals*, vol. 44, no. 2, pp. 541-567, 1995.

[13] A. G. Rehotn, J. Jiang, and P. E. Orban, "State-of-the-art methods and results in tool condition monitoring: a review," *The International Journal of Advanced Manufacturing Technology*, vol. 26, pp. 693-710, 2005.

[14] N. Ambhore, D. Kamble, S. Chinchanikar and V. Wayal, "Tool condition monitoring system: A review," in *Proceedings of the 4th International Conference on Materials Processing and Characterization*, 2015, pp. 3419-3428.

[15] D. A. Axinte, and N. Gindy, "Tool condition monitoring in broaching," *WEAR*, no. 254, pp. 370-382, 2003.

[16] P. J. Arrazola, J. Rech, R. M'Saoubi, and D. Axinte, "Broaching: Cutting tools and machine tools for manufacturing high quality features in components," *CIRP Annals - Manufacturing Technology*, vol. 69, pp. 554-577, 2020.

[17] A. Martini, A. Rivola, and M. Troncossi, "Autocorrelation Analysis of Vibro-Acoustic Signals Measured in a Test Field for Water Leak Detection," *Applied Sciences*, vol. 8, 2018.